Rare Metal Materials and Engineering
Volume 49, Issue 12, December 2020
Available online at www.rmme.ac.cn

Science Press

Cite this article as: Rare Metal Materials and Engineering, 2020, 49(12): 4088-4096.

ARTICLE

Growth Kinetics of Three-Dimensional Grains Based on Cellular Automata

Li Wei[1], Chu Zhibing[1,2], Wang Huanzhu[1], Su Hui[1], Xue Chun[1], Shuai Meirong[1], Li Yugui[1], Ma Lifeng[1]

[1] Engineering Research Center Heavy Machinery Ministry of Education, Taiyuan University of Science and Technology, Taiyuan 030024, China; [2] School of Mechanics and Civil Engineering, Jinan University, Guangzhou 510632, China

Abstract: Based on the thermodynamic conversion mechanism and energy transition principle, the three-dimensional (3D) grain growth process of AZ31 magnesium alloy was simulated by the improved cellular automata (CA) model of Metropolis algorithm, and the grain size and grain growth kinetics were analyzed. The simulation results show that CA model with the improved transformation rules is closer to the normal growth process of the actual 3D grain. In the simulation process, the total free energy of the system decreases, and the grain size presents normal distribution at different time. The grain diameter to average grain diameter (R/R_m) ratio stands at 1.0, which is the largest in grain distribution, and it satisfies the minimum energy criterion of grain evolution. The analysis of grain growth kinetics shows that the 3D grain growth process follows the relationship between average grain size and time during grain evolution, and the grain growth index is 0.479 41, which is close to the theoretical value of 0.5. The grain size variation of AZ31 magnesium alloy during heat preservation is also experimentally studied, verifying the reliability and accuracy of the 3D cellular automata model established in this research.

Key words: three-dimensional grains; evolution rules; grain size distribution; kinetics of grain growth

Grain growth has an important relationship with the mechanical properties of plasticity, strength and stiffness of polycrystalline materials. It is important to study the grain growth to improve the mechanical properties of materials. Generally, the observation of microstructure is usually characterized by metallographic, scanning electron microscope (SEM), transmission electron microscope (TEM) and electron backscattered diffraction (EBSD). However, due to the restricted experimental conditions, it is difficult to observe the actual grain growth process in real time[1]. Therefore, the computer simulation method for microstructure evolution is proposed to predict and research the grain growth process[2]. At present, the commonly used simulation methods include Monte Carlo (MC) method, cellular automata (CA) method and phase field (PF) method[3]. CA method is widely used in the simulation of crystallization and solidification, grain growth and recrystallization, phase precipitation, phase decomposition, dislocation and other processes, especially in the process of grain growth and recrystallization evolution[4].

In terms of grain growth, Liu et al[5] first simulated 2D grain growth process by combining CA method with MC method, and analyzed the size, edge number and growth kinetics of grain growth. Based on the grain boundary transition principle, Getger et al[6] improved the transition rules of CA to simulate the growth of 2D grains. In recent years, Ma et al[7] simulated grain growth at different temperatures through improved CA model. Wang et al[8] extended the 2D CA model to 3D, and studied various rules

Received date: December 08, 2019
Foundation item: National Key R&D Program (2018YFB1307902); National Natural Science Foundation of China (U1710113); China Post-doctoral Science Foundation (2017M622903); Shanxi Key R&D Project (201703D111003); Shanxi Province Graduate Joint Talent Training Project (2018JD33); Shanxi Graduate Education Innovation Project (2019SY482); Outstanding Young Academic Leader of Colleges and Universities in Shanxi Province (2019045); Shanxi Province Outstanding Achievement Cultivation Project (2019KJ027)
Corresponding author: Chu Zhibing, Ph. D., Professor, School of Materials Science and Engineering, Taiyuan University of Science and Technology, Taiyuan 030024, P. R. China, Tel: 0086-351-2776763, E-mail: piegen@163.com

and characteristics of 2D and 3D grain growth. Wang et al[9] simulated the growth process of 3D grains and studied their quasi-steady distribution through the improved Potts model through MC method. Similarly, the evolution process simulation of material microstructure is one of the hotspots for many scholars. Raabe et al[10] combined the CA method with the finite element (FE) method to study the 3D evolution of recrystallized grains, and discussed the coupling relationship between the CA and the crystal plastic FE model. Svyetlichnyy et al[11] proposed an improved 3D computer-aided design method, established a 3D CA model including grain deformation, recrystallization and grain growth after recrystallization, and considered the influence of temperature, strain, strain rate, dislocation density, crystal orientation and other parameters on the evolution process. Svyetlichnyy et al[12] proposed a process of microstructure evolution model based on 3D CA, obtained grain distribution by changing nucleation conditions and grain growth conditions, and studied the distribution of crystal orientation and boundary orientation angle. On the one hand, the above establishment of 3D model does not have a certain correlation with 2D model; on the other hand, due to the large amount of calculation, many scholars only studied the evolution model with FE method, but have no separate studies on grain growth process. Thus it has some limitation during the simulation when mapping from microcosmic to macroscopic scales.

In this research, a CA model improved by Metropolis algorithm was used to simulate the 3D grain growth process based on thermodynamic conversion mechanism and energy transition principle. The dynamics of grain size and grain growth under 3D conditions was studied, and the grain distribution of the model in the 2D section was studied by the slicing technique. Through the study of grain orientation and the visualization of grain growth, a method was provided for the study of grain orientation during grain growth. Finally, due to the restricted experimental conditions, this research indirectly verified the accuracy of the 3D model by comparing the grain size of the metallographic structure before and after the thermal insulation.

1 Experiment

AZ31 magnesium alloy supplied by Silver Magnesium Industry was used as billet. Its chemical composition is shown in Table 1.

The magnesium alloy was stored at 420 °C for 12 h, and subjected to a metallographic experiment before the thermal insulation. The original grain structure is shown in Fig.1.

2 Simulated Initial Conditions

2.1 Principle of 3D CA method

The modeling method of 3D CA generally adopts the top-down method, whose essence is to discretize the complex change process of grains in continuous time and continuous space, and formulate the corresponding deterministic or probabilistic cellular transformation rules to simulate the complex process of the interaction between adjacent cellulars[13]. The model has three dimensions of cellular space, which is in good consistency with the dimension of grain evolution process, and can intuitively represent the actual process of grain evolution.

Table 1 Chemical composition of as-cast AZ31 magnesium alloy (wt%)

Al	Mn	Zn	Ca	Ni	Fe	Si	Mg
2.5~3.5	0.15~0.5	0.6~1.4	0.05	0.005	0.005	0.1	Bal.

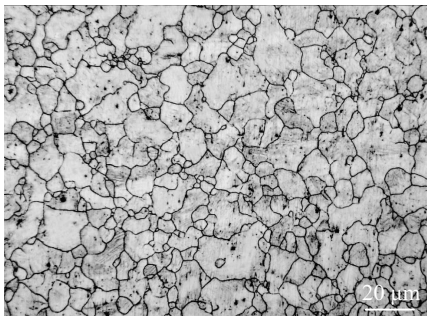

Fig.1 Original grain structure of AZ31 magnesium alloy

The 3D CA consists of five main parts, including cellular, cellular space, cellular state, cellular neighborhood type and transition rule.

(1) Cellular

Cellular is the basic element of CA. According to the geometric shape, the 3D model can be divided into octahedral cellular, cube cellular and sphere cellular. In this research, cube cellular is adopted.

(2) Cellular state

Cellular state can carry multiple cellular variables. In this research, cellular adopts two kinds of state variables. The first variable is a grain oriented variable with a random integer of 1~180. The same grain orientation variable represents the same grain, and the cellular simulates the transition of atoms between different grains by the change of grain orientation variable. The second variable is grain boundary variables. Grain boundary variables can judge whether the cellular is in grain boundary, i.e., whether the cellular belongs to the grain boundary cellular or the internal cellular. If the grain boundary variable is 0, it means the internal cellular; if the grain boundary variable is 1, it means the grain boundary cellular. The edge length of the cellular adopted in this research is 2 μm.

(3) Cellular space

The set of space in which cells are located is called cellular space. Cellular space is usually divided into 1D space, 2D space, 3D space and multi-dimensional Euclidean space. In this research, 3D space was used to simulate the changes of grains in local intervals. The simulated area was 0.4 mm×0.4

mm×0.4 mm. In other words, the simulated area was composed of 200×200×200 3D cube cellulars. Because the grain size is several orders of magnitude smaller than the workpiece size, considering the running ability of the computer, the boundary conditions must be set to reduce the computer computation. Generally, boundary conditions can be divided into periodic boundary conditions, reflective boundary conditions and fixed value boundary conditions. 3D periodic boundary conditions connect up and down, left and right, and back and forth, which can be used to approximately simulate an infinite area. As shown in Fig.2, 3D periodic boundary conditions are adopted in this research.

(4) Cellular neighborhood type

The state of the cellular at the next moment is not only associated with its own state, but also closely related to the cellular neighbors around the state. The more neighbors, the more accurate the model, and the larger the amount of computations. In order to improve the accuracy of the models, this research adopts 3D Moore neighbor type, as shown in Fig.3. In 3D Moore neighbors, the state of the central cellular in the next CA step (CAS) is determined by the state of the 26 neighbors in the current CAS, i.e., the state of the nearest 6 neighbors, the next 12 neighbors and the furthest 8 neighbors[14].

(5) Cellular transition rule

The transition rule in CA is a key factor, which directly determines the final shape of simulation, to judge the cellular state in the next CAS according to the neighbor cellular state in the current step.

2.2 Cellular transition rule

According to the physical mechanism of grain growth and the principle of energy transition, this research established the transition rule of CA for the normal growth of 3D grains through the probabilistic transition rule of thermodynamic energy fluctuation. The improved transition rule is as follows.

(1) Traverse all cellulars and find the ones at the grain boundary. The grain boundary of each cellular can be expressed by the Hamilton function[15], which is used to express the interaction between atoms. Calculate the grain boundary energy E_i between the cellular and the surrounding cellular:

$$E_i=\gamma\sum_{i=1}^{N}\sum_{j=1}^{M}(1-\delta_{s_is_j}) \tag{1}$$

$$\delta_{s_is_j}=\begin{cases}1, & S_i=S_j\\ 0, & S_i\neq S_j\end{cases} \tag{2}$$

where γ is a positive grain boundary energy constant (assuming that when the grain growth is isotropic, γ is 1); N is the number of grain orientations; M is the number of all neighbors of cellular i (26 is taken); S_i and S_j are the number of grain orientations of cellular i and cellular j, respectively; $\delta_{s_is_j}$ is a Kronecker δ function.

(2) Find a cellular in the neighbor cellular that is different from the cellular orientation number, and randomly assign a new orientation number to the neighbor cellular. Calculate the new grain boundary energy of the cellular after the transition E_{i+1}.

(3) The grain gradually reaches a steady state during the growth process, and the total energy of the system gradually decreases. The variation of the grain boundary energy of the system is consistent with the change of the grain boundary energy of the cellular, which can be expressed as $\Delta E=E_{i+1}-E_i$. The energy difference after transformation is judged. If $\Delta E\leqslant 0$, the cellular will undergo transformation, i.e., the transformation probability is 1; if $\Delta E>0$, the cellular will be judged by the energy transition principle.

(4) According to the principle of energy transition, if $\Delta E>0$, a probabilistic transition rule is established. Grain growth is actually the process of continuous transition of grain boundary atoms. Fig.4 shows the energy conversion process of atoms from one grain to another. The energy required for transition from grain 1 to grain 2 is ΔE_{A}, and the energy

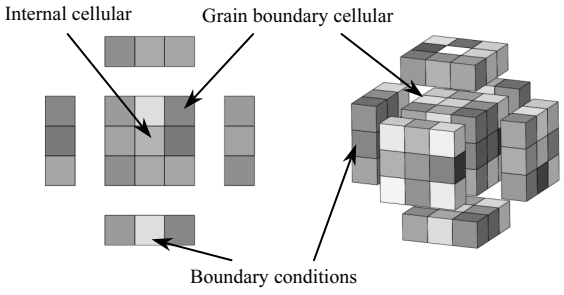

Fig.2 3D periodic boundary conditions

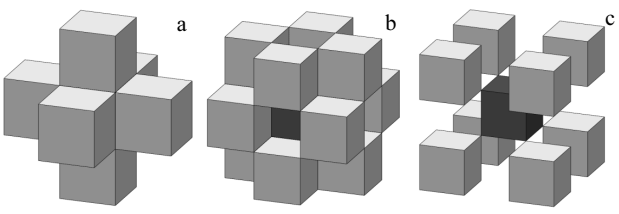

Fig.3 6 (a), 12 (b), and 8 (c) neighbors of 3D Moore neighbor type

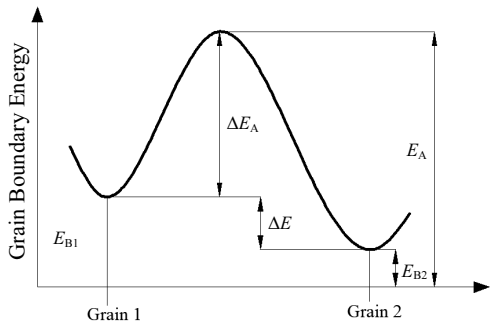

Fig.4 Energy transformation of the atom during the transition process

required for transition from grain 2 back to grain 1 is $\Delta E_A + \Delta E$, where $\Delta E = E_{B1} - E_{B2}$, E_{B1} and E_{B2} represent the grain boundary energy of grain 1 and grain 2, respectively[16].

The probability of atom transition from grain 1 to grain 2 is

$$P_1 = \exp(-\Delta E_A / RT) \quad (3)$$

The probability of atom transition from grain 2 back to grain 1 is

$$P_2 = \exp(-(\Delta E_A + \Delta E)/RT) \quad (4)$$

where T is the absolute temperature, and R is the gas constant. The final probability of atom transition from grain 1 to grain 2 can be expressed as follows:

$$P = P_1 - P_2 = P_1(1 - P_3) \quad (5)$$

where $P_3 = \exp(-\Delta E/RT)$. During the transition of each step of the CA, each cellular is transformed according to the probability P.

Therefore, the final transformation rule of cellular can be expressed as follows:

$$W = \begin{cases} 1, \ \Delta E \le 0 \\ P, \ \Delta E > 0 \end{cases} \quad (6)$$

In the CA method, each cell of the lattice represents a group of atoms, and the evolution of the microstructure is governed by the behavior of individual cells acting in response to their neighborhoods. The maximum number of grain orientation determines the resolution of the simulation, depending on the computer power available.

The significance of the improved transformation rule is that the cellular with the change of grain orientation is located at the grain boundary. In the process of 3D grain transformation, in order to meet the principle of boundary flattening in the process of actual grain growth, this rule gives priority to the thermodynamic transformation mechanism, i.e., if the total grain boundary energy of the system decreases after the transformation, the cellular will be transformed; otherwise, the cellular will not be transformed. When the cellular does not meet the thermodynamic conversion mechanism, the energy transition principle is used to judge. In other words, one of the 26 neighboring cellulars is randomly selected, and then judged according to whether it meets the principle of total grain boundary energy reduction of the system. The improved transformation rule makes the CA model closer to the actual 3D grain growth process, and improves the reliability and accuracy of the simulation.

2.3 Normal growth process of 3D grains

Fig.5 shows the flow chart of grain growth simulation at a certain time.

Step 1: input parameters. The initial cellular space and grain orientation number are given to the cellular. The cellular space is used to determine the size of the simulated real space, and the grain orientation number is used to describe the different grains and distinguish the internal cellular from grain boundary cellular.

Step 2: the initial CAS tt=1. The transition probability P of the cellular at this CAS is calculated and random number 0 or 1 is assigned to the cellular.

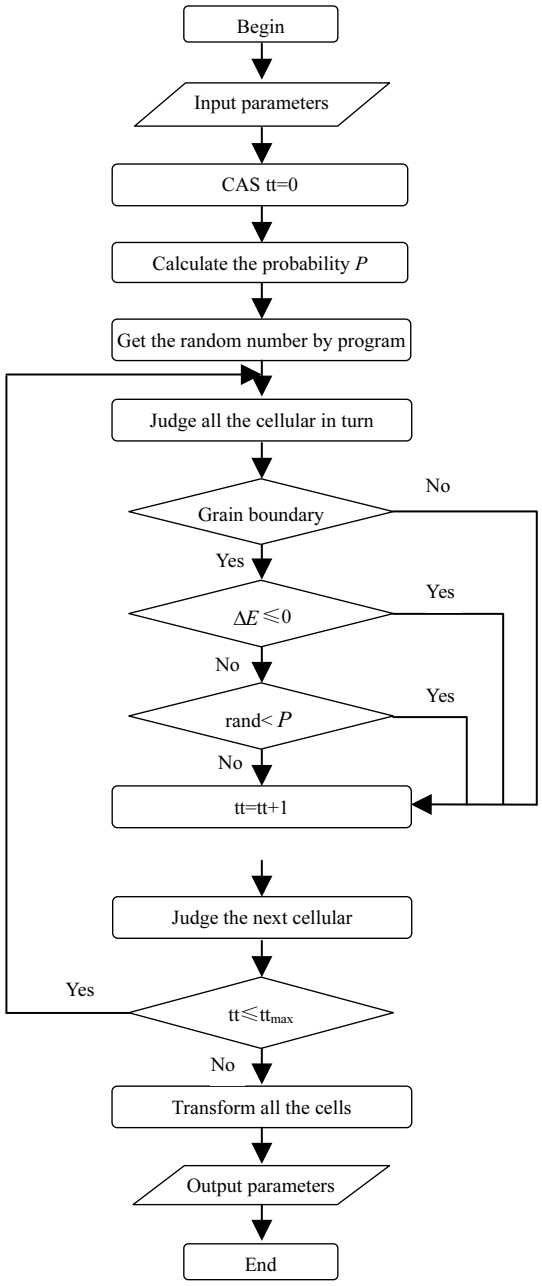

Fig.5 Flow chart of grain growth simulation

Step 3: determine whether it is grain boundary cellular. By comparing the size of random number rand and transformation probability P, we can determine whether the cellular is likely to undergo transformation.

Step 4: the cellular that may be transformed is determined by Step 3, and whether the cellular satisfies $\Delta E \leqslant 0$ or rand<P is determined successively.

Step 5: traverse all the cellulars. Each cellular undergoes Step 3 and 4, and the cellular satisfying the rules is transformed. At this time, tt=tt+1. Go to the next CAS and judge the entire

cellular. In the process of growing up, it is necessary to repeat the process continuously to make the grain grow up.

3 Results and Discussion

3.1 3D grain growth simulation

Fig.6 shows the initial 3D grain structure of simulated by the CA model. By observing the initial structures obtained in this simulation, it can be seen that the distribution of grains in the three directions of *X*, *Y* and *Z* is relatively stable, the grain orientation is in a random distribution state, and the grains with different orientations are mapped into different colors. 3D slices are made along the *Y*-axis to obtain the 2D distribution of the initial grain structure. By comparing the grain structure of each slice layer, it can be found that the random distribution in the direction of *X*, *Y* and *Z* is also realized inside the grain, which indicates that the model successfully achieves the establishment of 3D model by combining the cellular with its neighbors.

The surface of the 3D model can be seen as a section of the 2D model (Fig.7). By observing the cross section diagrams at different time, it can be known that the intersection angle of grains at the intersection of three intersecting grains at the 2D section is approximately equal to 120°. With the increase of CAS, grains with intersection angle smaller than 120° are gradually devoured, while grains with intersection angle larger than 120° grow after collision with surrounding grains. This is because grain boundaries tend to be flat in order to minimize local free energy during grain growth. Large grains gobble up small grains, which reduces the total free energy of the system and satisfies the grain boundary flattening principle. Finally, stable grains with a grain edge number of 6 are presented in the 2D plane, which satisfies Neumann model[17]:

$$\frac{\mathrm{d}A}{\mathrm{d}t}=\frac{\pi}{3}m\gamma(n-6) \tag{7}$$

where n is the number of crystal grains, the grain boundary mobility m and the interface energy γ are proportional constants, t is grain growth time, and A is the crystal grain area. This formula reveals the quantitative relationship between the grain growth rate and the topological parameters of the grains (the number of grain edges n).

According to the transformation rules, the 3D grain growth is obtained by iterating between the cellular and 26 neighboring cellulars. As shown in Fig.8a~8d, the instantaneous diagrams of grain growth of different orientations at CAS of 500, 1000, 1500 and 2000 are shown, respectively. In order to observe the grain growth rule and form it more conveniently, the grain boundaries are extracted separately as shown in Fig.8e~8h.

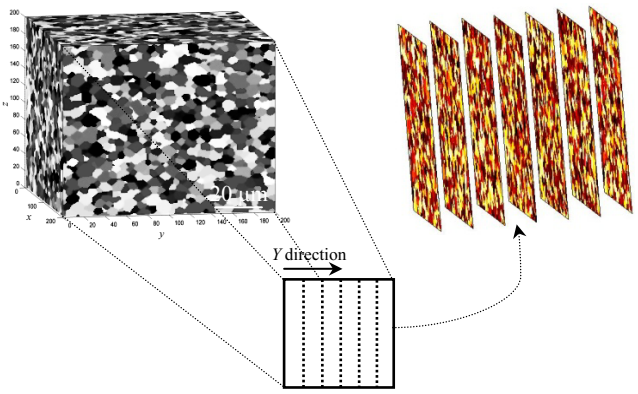

Fig.6 3D grain initial structure

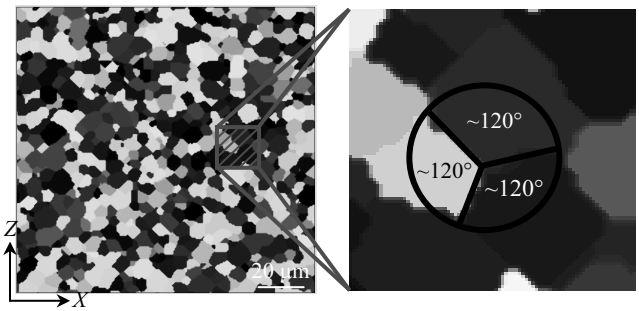

Fig.7 Angle between 2D section grain boundaries

Fig.9 shows the number of grains in different CAS. As the CAS increases, the number of grains decreases significantly. The grain size increases significantly when grain number decreases from 2716 to 876. It can be seen from the slope that the grain growth rate becomes slower and slower, indicating that the grain growth tends to be more and more stable, and the grain growth is gradually completed.

In order to further observe the growth process of grains, grains with orientation number Q=5 are extracted separately, as shown in Fig.10. It can be seen from the figure that the grain grows significantly in the 3D space, and its morphology is approximately "spherical" or "ellipsoidal" during the growth process. There are three main growing forms of grains: growing grains, disappearing grains and devouring smaller grains in the growing process, corresponding to Fig.11a, 11b and 11c, respectively. As the CAS progresses, some grains grow gradually, while some larger grains devour the smaller ones and then grow. This is because the simulated space remains unchanged during the growth of grains, and some grains will gradually disappear during the normal growth of grains, which conforms to the principle of volume invariability during the growth of grains. At the same time, the growth and disappearance of single grain are observed as a result of changes of the grain orientation variables inside the cellular at the grain boundary location.

3.2 Grain size statistics

Grain size distribution is an important indicator to reflect the uniformity of grain distribution in the growth process of microstructure, and it is also the most important quantitative parameter to describe the internal structure characteristics of

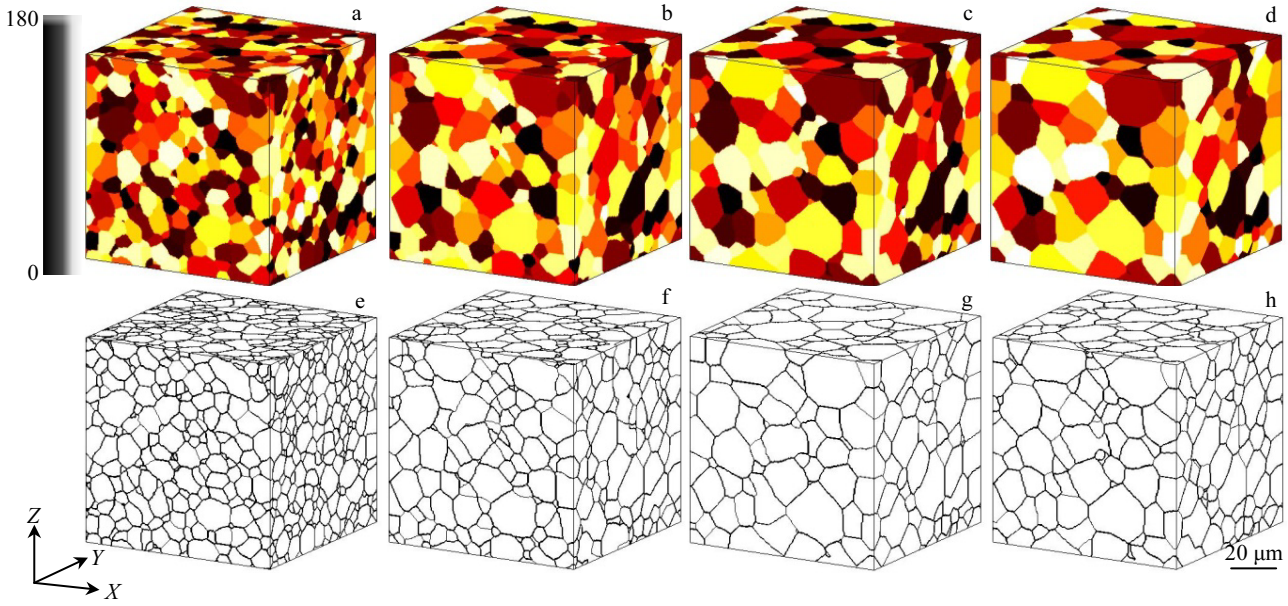

Fig.8 3D grain orientation and grain boundary diagrams at different CAS: (a, e) 500, (b, f) 1000, (c, g) 1500, and (d, h) 2000

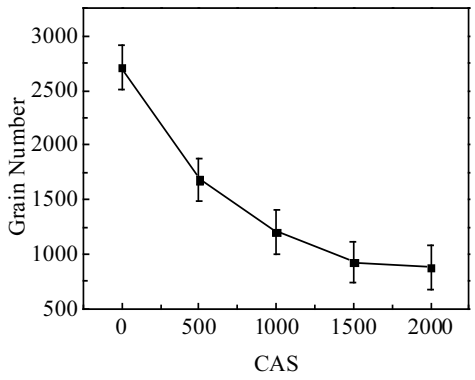

Fig.9 Grain number at different CAS

grain during the growth process[18]. It is usually expressed by the ratio of grain diameter to average grain diameter, namely R/R_m. Fig.12 intuitively shows the distribution of 3D grain size at different time steps. Through the GaussAmp nonlinear fitting of grain size, it can be found that with the increase of CAS, the average grain size increases, and the distribution of grain size basically conforms to the normal distribution, among which the distribution of R/R_m approaching 1.0 is maximized, and the proportion of R/R_m less than 0.5 or more than 2.5 is almost none. It indicates that there are few larger or smaller grains in the simulated grains, which is in line with the normal grain growth rule. This result satisfies the minimum energy criterion of grain evolution[19], which further verifies the correctness of the 3D CA model.

3.3 Kinetics analysis of grain growth

Normal grain growth satisfies the grain growth dynamics

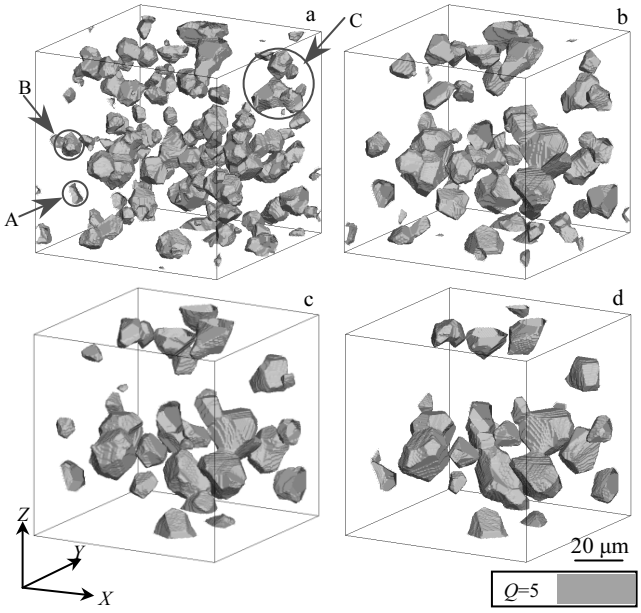

Fig.10 Grain growth process with orientation number Q=5 at different CAS: (a) 500, (b) 1000, (c) 1500, and (d) 2000

formula proposed by Beck et al[20], which describes the parabolic relation of average grain size changing with time in the process of grain evolution, expressed as follows:

$$R_m = Ct^n \quad (8)$$

where R_m is the average grain size, C is the system constant related to temperature and material, t is the isothermal annealing time, namely the simulation CAS, and n is the grain growth index, namely the kinetic time index. Many scholars

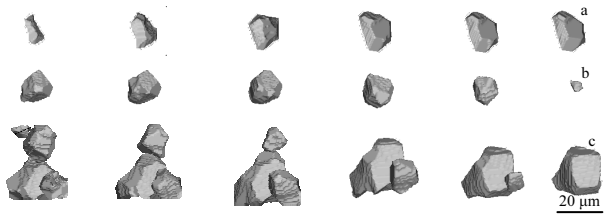

Fig.11 Main growth forms of grains A~C marked in Fig.10a under the same orientation number: (a) growing grain A, (b) disappearing grain B, and (c) devouring smaller grain C

have repeatedly proved that the theoretical value of n during normal grain growth is equal to 0.5[21,22].

Take the logarithm on both sides of Eq.(8):

$$\ln R_{\mathrm{m}} = \ln C + n \ln t \tag{9}$$

In this research, the average grain size is calculated once every 10 CAS and the slope of the curve obtained by linear fitting $\ln R_{\mathrm{m}}$-$\ln t$ is the value of the grain growth index n. Fig.13a shows the linear fitting result from the initial CAS of 10 to 2000. The growth index n is 0.457 63. By observing the experimental results, the deviation is larger in the CAS range of 0 to 100. This is due to the instability in the early stage of grain growth. After removing the results of the first 100 CAS, the results in the CAS from 100 to 2000 are fitted. As shown in Fig.13b, a new grain growth index n is 0.479 41, which is very close to the theoretical value of 0.5.

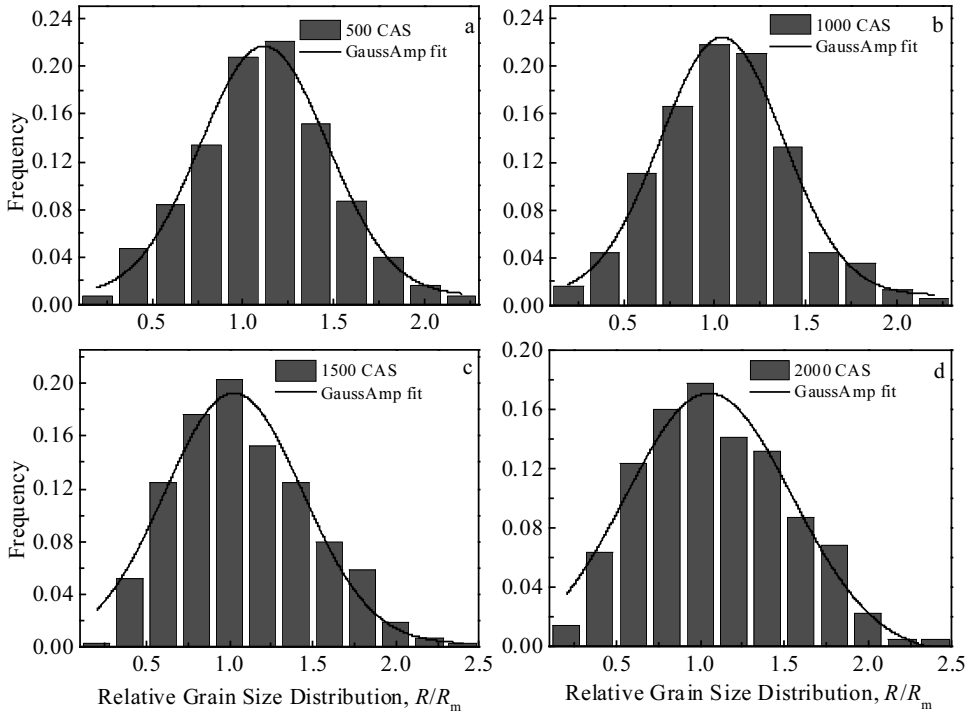

Fig.12 Grain size distribution at different CAS: (a) 500, (b) 1000, (c) 1500, and (d) 2000

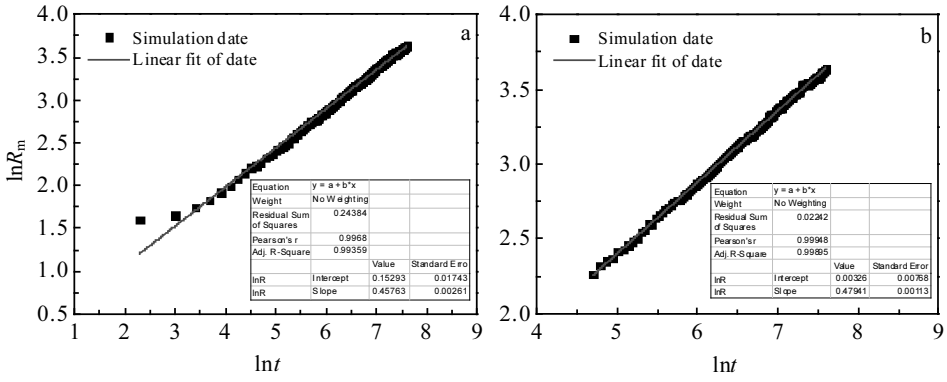

Fig.13 $\ln R_{\mathrm{m}}$-$\ln t$ curves and its linear fit results of the average grain size as a function of the simulation CAS: (a) 10~2000 CAS and (b) 100~2000 CAS

3.4 Grain topology analysis

The normal growth of the three-dimensional grain satisfies the Aboav-Weaire equation[23-25], which describes the relationship between the number of grain faces f and the average number of faces m_f of its nearest neighbor grains:

$$m_{\mathrm{f}} = < f > -1 + \frac{< f > + \mu_2}{f} \quad (10)$$

where μ_2 is a variance of the number of crystal facets, and $<f>$ is an average value of the number of three-dimensional crystal faces f.

In this research, according to the number of grains with different orientations around a grain, the number of grain faces is determined. The results show that the average grain surface is between 12 and 14, and the maximum grain surface is over 40.

3.5 CAS and real time correspondence

In order to make the simulated CAS in the established 3D CA model correspond to the time in real space, this research refers to the corresponding relationship between simulated time and real time used by Radhakrishnan et al[26] in the Monte Carlo model:

$$\mathrm{CAS} = \frac{At}{\exp(B/T)} \quad (11)$$

where T is the temperature, t is the real time, CAS is the simulated time, A and B are constants.

The simulation results and experimental conditions at different temperatures are selected and fitted to establish a relational formula suitable for this model, from which A=2868.006 and B=1190.570 can be obtained.

3.6 Experimental verification

Due to the long period and high cost of 3D characterization technology, this research uses 2D metallography to verify the simulation results indirectly. After 12 h insulation at 420 °C, the microstructure of the grain is shown in Fig.14. By comparing the metallographic structure before and after insulation, it can be seen that grain growth occurs in the original structure, grain boundary tends to be straight and adjacent grain angle is 120°, which is consistent with the conclusion obtained by simulation results.

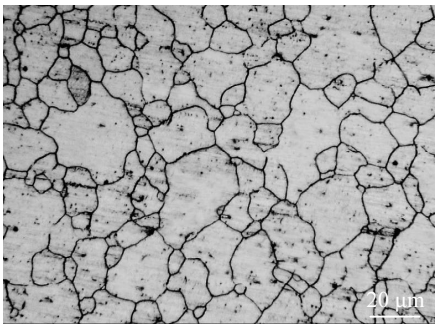

Fig.14 Grain structure after 12 h preservation at 420 °C

Table 2 Experimental and simulated grain size at different temperatures

Temperature/°C	Grain size/μm	
	Measured	Predicted
Room temperature	5.9	5.6
420	21.8	21.2

The grain size before and after the insulation is measured by the cross-section method and compared with the simulation results, as shown in Table 2. The error of the two is 0.3~0.6 μm, which indicates that the established 3D CA model can well simulate the grain growth process of AZ31 magnesium alloy.

4 Conclusions

1) Based on the thermodynamic conversion mechanism and the principle of energy transition, this research uses the improved CA model of Metropolis algorithm to establish a 3D CA model of grain growth for AZ31 magnesium alloy. Through the 3D slicing of the initial grain structure, the distribution of the model in the 3D direction is realized, and the angle and the number of crystal grains on the section of the slice are analyzed. The obtained results are consistent with the conclusions of the 2D CA model.

2) The 3D grain size distribution is studied. Through Gauss-Amp nonlinear fitting of grain size, grain size distribution conforms to normal distribution, among which R/R_{m} approaching 1.0 has the largest grain distribution. It conforms to the law of normal grain growth and meets the minimum energy criterion of grain evolution.

3) The grain growth kinetics is analyzed, and the 3D grain growth index n within CA step of 100~2000 is 0.479 41, which is very close to the theoretical value of 0.5. It satisfies the grain growth kinetics formula.

4) The grain growth phenomenon of AZ31 magnesium alloy during heat preservation can be observed through experiments, and the grain size is counted, which verifies the correctness of the simulation results.

References

1 Ding H L, He Y Z, Liu L F *et al. Journal of Crystal Growth*[J], 2006, 293(2): 489

2 Anderson M P, Srolovitz D J, Grest G S *et al. Acta Metallurgica*[J], 1984, 32(5): 783

3 Li Xing, Fang Bin, Xu Xiuguo *et al. Materials Reports*[J], 2011, 25(2): 245 (in Chinese)

4 Zhu Peipei. *Thesis for Master*[D]. Harbin: Harbin Institute of Technology, 2016 (in Chinese)

5 Liu Y, Baudin T, Penelle R. *Scripta Materialia*[J], 1996, 34(11): 1679

6 Geiger J, Roósz A, Barkóczy P. *Acta Materialia*[J], 2001, 49(4): 623

7 Ma Xiaofei, Guan Xiaojun, Liu Yunteng *et al. The Chinese*

Journal of Nonferrous Metals[J], 2008, 18(1): 138 (in Chinese)
8 Wang Hao. *Thesis for Master*[D]. Taiyuan: Taiyuan University of Technology, 2014 (in Chinese)
9 Wang Hao, Liu Guoquan, Qin Xiangge. *Rare Metal Materials and Engineering*[J], 2009, 38(1): 126 (in Chinese)
10 Raabe D. *Annual Review of Materials Research*[J], 2002, 32(32): 53
11 Svyetlichnyy D S, Matachowski J L. *AIP Conference Proceedings*[C]. Porto: American Institute of Physics, 2007, 908(1): 1357
12 Svyetlichnyy D S. *Modelling & Simulation in Materials Science and Engineering*[J], 2014, 22(8): 85 001
13 Wang Min, Zhou Jianxin, Yin Yajun *et al. Metallurgical & Materials Transactions B*[J], 2017, 48(5): 2245
14 Guo Dongxu. *Thesis for Master*[D]. Yinchuan: Ningxia University, 2014 (in Chinese)
15 Yuan Ranxu. *Thesis for Master*[D]. Harbin: Harbin Institute of Technology, 2017 (in Chinese)
16 He Y Z, Ding H L, Liu L F *et al*. *Materials Science and Engineering A*[J], 2006, 429(1-2): 236
17 Mao Weimin. *Recrystallization and Grain Growth of Metals*[M]. Beijing: Metallurgical Industry Press, 1994: 307 (in Chinese)
18 Zhang Jie. *Thesis for Master*[D]. Beijing: General Research Institute for Nonferrous Metals, 2018 (in Chinese)
19 Li Xu. *Thesis for Master*[D]. Nanjing: Nanjing University of Aeronautics and Astronautics, 2012 (in Chinese)
20 Beck P A, Holzworth M L, Hu H. *Physical Review*[J], 1948, 73(5): 526
21 Radhakrishnan B, Zacharia T. *Metallurgical and Materials Transactions A*[J], 1995, 26(1): 167
22 Zhang Jixiang, Guan Xiaojun, Sun Sheng *et al. Journal of Shandong University (Engineering Science)*[J], 2005, 35(4): 1 (in Chinese)
23 Aboav D A. *Metallography*[J], 1970, 3(4): 383
24 Edwards S F, Pithia K D. *Physica A Statistical Mechanics & Its Applications*[J], 1994, 205(4): 577
25 Xue Weihua. *Thesis for Doctorate*[D]. Beijing: University of Science and Technology Beijing, 2017
26 Radhakrishnan B, Zacharia T. *Metallurgical and Materials Transactions A*[J], 1995, 26(8): 2123

基于元胞自动机的三维晶粒长大动力学研究

李　伟[1]，楚志兵[1,2]，王环珠[1]，苏　辉[1]，薛　春[1]，帅美荣[1]，李玉贵[1]，马立峰[1]
(1. 太原科技大学 重型机械教育部工程研究中心，山西 太原 030024)
(2. 暨南大学 力学与建筑工程学院，广东 广州 510632)

摘　要：基于热力学转换机制和能量跃迁原理，采用 Metropolis 算法改进的元胞自动机模型，对 AZ31 镁合金三维晶粒长大过程进行仿真研究，并对其晶粒尺寸与晶粒长大动力学进行统计分析。仿真结果表明：采用改进转变规则后的元胞自动机模型更加接近于实际三维晶粒的正常长大过程。在模拟过程中，系统总自由能降低，不同时刻晶粒尺寸均呈现正态分布。晶粒直径与平均晶粒直径的比值 $R/R_m \approx 1.0$ 的晶粒分布最多，满足晶粒演变最小能量准则。分析晶粒长大动力学可知，三维晶粒长大遵循晶粒演变过程中平均晶粒尺寸随时间变化的关系，晶粒长大指数为 0.479 41，非常接近于理论值 0.5。通过实验对 AZ31 镁合金保温过程中晶粒尺寸变化规律进行研究，验证了建立的三维元胞自动机模型的可靠性与准确性。

关键词：三维晶粒；转变规则；晶粒尺寸分布；晶粒长大动力学

作者简介：李　伟，男，1994 年生，硕士生，太原科技大学材料学院，山西 太原 030024，电话：0351-2776763，E-mail: 854523935@qq.com